Electronic Supplementary Information

Heterogenous Cu@ZrO_2 nanofibers enable efficient electrocatalytic nitrate reduction to ammonia under ambient conditions

Jiaojiao Xia, [a,b] Hongting Du, [b] Shuyue Dong, [b] Yongsong Luo, [b] Qian Liu, [a] Jun Song Chen, [b] Haoran Guo*[c] and Tingshuai Li*[b]

[a] Institute for Advanced Study, Chengdu University, Chengdu, 610106, Sichuan, China

[b] School of Materials and Energy, University of Electronic Science and Technology of China, Chengdu, 611731, Sichuan, China

[c] School of Chemical Sciences, University of Chinese Academy of Sciences, Yuquan Road, Shijingshan District, Beijing, 100049, China

*Corresponding authors: GuoHRan@163.com and litingshuai@uestc.edu.cn

Calculation method

First-principles calculations are performed using the Vienna Ab initio Simulation Package (VASP) [1-3] to investigate the NO_3^-RR process on the CLZ surfaces. The valence-core electrons interactions are treated by Projector Augmented Wave (PAW) [4] potentials and the electron exchange correlation interactions are described by the generalized gradient approximation (GGA) with the Perdew-Burke-Ernzerhof (PBE) [5] functional. Considered long-range interaction at the interface, Van der Waals interactions are considered using DFT-D3 correlation [6]. To avoid interaction from other slabs, a vacuum of 20 Å is added along z direction. The convergence criterion of geometry relaxation is set to 0.03 eV•Å^{-1} in force on each atom. The energy cutoff for plane wave-basis is set to 500 eV. The K points are sampled with 3×3×1 by Monkhorst-Pack method [7].

Gibbs free energy change (ΔG) is evaluated based on the computational hydrogen electrode (CHE) model, which takes one-half of the chemical potential of gaseous hydrogen under standard conditions as the free energy of the proton-electron pairs. ΔG is calculated by the following equation [8]:

$$\Delta G = \Delta E + \Delta E_{ZPE} - T\Delta S + neU \quad (1)$$

where ΔE, ΔE_{ZPE}, ΔS are the reaction energy from DFT calculation, the correction of zero-point energy and the change of simulated entropy, respectively. T is the temperature (T=300 K). *n* and U are the number of transferred electrons and applied potential respectively.

Experimental Method

Materials： Disodium phosphate (Na_2HPO_4), sodium dihydrogen phosphate (NaH_2PO_4), Zirconium acetate ($C_8H_{12}O_8Zr$) and polyvinylpyrrolidone (PVP) are purchased from Aladdin Ltd (Shanghai, China). Sulfanilamide ($C_6H_8N_2O_2S$) is bought from Heowns technology Co., Ltd. N,N-Dimethylformamide (DMF), sodium nitrate ($NaNO_3$), sodium nitrite ($NaNO_2$), N- (1-naphthyl) ethyl diamine dihydrochloride ($C_{12}H_{14}N_2$.2(HCl)), copper (II) nitrate trihydrate (Cu $(NO_3)_2 \cdot 3H_2O$), phosphoric acid (H_3PO_4), ammonium chloride (NH_4Cl), sodium hypochlorite solution (NaClO), 4-dimethylaminobenzaldehyde ($C_9H_{11}NO$), sodium nitroferricyanide dihydrate ($C_5FeN_6Na_2$-O$\cdot 2H_2O$), hydrazine monohydrate ($N_2H_4 \cdot H_2O$), hydrogen peroxide (H_2O_2, 3 wt%), hydrochloric acid (HCl), sulfuric acid (H_2SO_4), sodium hydroxide (NaOH) potassium hydroxide (KOH), salicylic acid ($C_7H_6O_3$), trisodium citrate dihydrate ($C_6H_5Na_3O_7$- $2H_2O$) and ethanol (C_2H_5OH) are purchased from Kelong chemical Ltd (Chengdu, China). Sodium salicylate ($C_7H_5NaO_3$) is purchased from Fuchen chemical reagents Co., Ltd (Tianjin, China). Nafion solution (5 wt%) is purchased from Sigma-Aldrich Chemical Reagent Co., Ltd. Deionized water is purified through a Millipore system.

Synthesis of Cu-Doped-ZrO_2 nanofibers: 2.8 g of PVP (Mw=1,300,000 g mol^{-1}) and 0.7 g of $Cu(NO_3)_2 \cdot 3H_2O$ are dissolved in 20 mL of mixture solution including DMF and $C_8H_{12}O_8Zr$ (a volume ratio of 8:2), and then this viscous solution is uniformly stirred for 12 h. After that, the mixture is spun into nanofibers at a high voltage of 15 kV. After electrospinning, the fibers are collected to be heat treated at 350 °C for 1 h and consecutively sintered at 800

°C for 3 h, which can naturally cool to room temperature to get the Cu-Doped-ZrO_2 nanofibers.

Synthesis of Cu-Loaded-ZrO_2 nanofibers: ZrO_2 nanofibers are synthesized by following the above route [9]. Subsequently, 0.8 g of ZrO_2 and 0.3 g of $Cu(NO_3)_2 \cdot 3H_2O$ are dissolved into 10 ml of deionized water. Then, the above turbid solution is magnetically stirred for 28 h at room temperature. Afterward, this entire solution is dried at 110 °C for 10 h in the vacuum-drying oven. At last, the sample is placed in a tube furnace and sintered at 450 °C for 3 h in a 5% v/v H_2/Ar atmosphere. Therefore, the metal state of Cu at the surface of ZrO_2 nanofibers is obtained.

Material characterizations： X-ray diffraction (XRD) analysis is performed by a Rigaku Smartlab with the radiation of Cu Kα. The sample morphology is photographed by ZEISS Gemini SEM 300 scanning electron microscope. The acceleration voltage is 3 kV during topography shooting and 15 kV during energy spectrum mapping shooting. The detector is SE2 secondary electronic detector. The transmission electron microscopy (TEM) and high-resolution TEM (HRTEM) images of sample are obtained from FEI F30 equipment with the accelerating voltage of 300 kV. X-ray photoelectron spectrometer (Thermo Fischer, ESCALAB Xi+) is used for the test XPS of catalysts. The excitation source is Al Ka ray (hv =1486.6 eV), and the working voltage is 12.5 kV. Nuclear magnetic resonance (NMR) is measured on a Bruker 400 MHz instrument. The elemental analysis is tested by ICP-OES (Agilent ICPOES730).

Working electrode preparation

5 mg catalyst were grinded into powder and added into a mixed solution containing 655 μL ethanol, 325 μL deionized water and 20 μL of 5 wt% Nafion solution, followed by 30 min ultrasonic dispersion to form a homogeneous suspension. Then, 20 μL of such suspension was dropped on a 1×1 cm^2 carbon paper and dried in ambient temperature.

Electrochemical measurements: All electrochemical tests were performed in an H cell with a Nafion membrane in the middle. A three-electrode system was used in the experiments. The working electrode was carbon sheet coated with catalyst, and the counter electrode was graphite rod. The electrolyte of the anode is the same as that of the cathode. The reference electrode was affected by the pH of the electrolyte. When the electrolyte is neutral, the reference electrode is saturated with Ag/AgCl/KCl. When the electrolyte is alkaline, the reference electrode is Hg/HgO/saturated KOH. The neutral electrolyte is 0.1 M PBS (prepared by Na_2HPO_4 and NaH_2PO_4) solution with pH=7, and the alkaline electrolyte is 0.1 M KOH solution with pH=13. $NaNO_3$ was added to the electrolyte after high temperature impurity removal as the N source.

In 0.1 M PBS+0.1 M $NaNO_3$ electrolyte, the voltage of the relative reference electrode (Ag/AgCl) is converted into the voltage of the relatively reversible hydrogen electrode (RHE) by formula (2):

$$E(vs.\ RHE) = E(vs.\ Ag\ /\ AgCl) + 0.552\ V \quad (2)$$

In 0.1 M KOH+0.1 M $NaNO_3$ electrolyte, the voltage of the relative reference electrode (Hg/HgO) is converted into the relatively reversible hydrogen electrode

voltage (RHE) by formula (3):

$$E(vs.\ RHE) = E(vs.\ Hg / HgO) + 0.865\ V \quad (3)$$

Linear sweep voltammetry (LSV) was used to compare the same electrolyte with and without nitrate at 5 mV S^{-1} scanning speed. Meanwhile, since nitrate concentration has a significant impact on NO_3RR process, LSV in the same electrolyte with different concentrations of nitrate was tested. Cyclic voltammetry (CV) tests were performed from 0.0 V to 0.1 V vs. Ag/AgCl at different scan rates of 20 mV s^{-1}, 40 mV s^{-1}, 60 mV s^{-1}, 80 mV s^{-1} and 100 mV s^{-1} without faradaic current. Solution resistance was determined by electrochemical impedance spectroscopy (EIS) at frequencies ranging from 0.1 to 10 kHz.

Determination of ammonia (NH_3): Ammonia produced in the NO_3^-RR process is colored by indophenol blue method [10] and detected by the UV-vis spectroscopy. Due to the high concentration of the product, all electrolytes after electrolysis are diluted 10~20 times before color development. After 1 hour of electrolysis, 2 mL electrolyte is taken from the cathode cell, followed by 2 mL colorant (containing salicylic acid, sodium citrate and sodium hydroxide), 1 mL oxidant (0.05 M sodium hypochlorite), and 0.2 mL catalyst solution (1 wt% sodium nitroferricyanide). Then, they are placed in the dark environment for 1 h, and the UV-vis spectra are measured in the wavelength range of 550 ~ 800 nm. The absorption intensity at 655 nm is substituted into the standard curve to quantify the ammonia yield.

Determination of nitrite (NO_2^-): The concentration of nitrite is measured by Griess reagent [11]. 0.2 g of N- (1-naphthyl) ethyl-diamine dihydrochloride, 2.0 g of sulfa

and 5.88 mL of phosphoric acid are dissolved in 100 mL of deionized water, and the Griess reagent is formed after being evenly stirred. After diluting the reacted electrolyte 10-20 times, 1 mL of the diluted electrolyte is taken by addition of 1 mL of Griess reagent and 2 mL of deionized water, and develop color stands in the dark environment of room temperature for 10 minutes. Magenta solution is obtained and UV-vis absorption spectra are tested in the ranges from 400 to 650 nm. The absorbance at 540 nm is substituted into the standard curve to obtain the concentration of nitrite.

Determination of hydrazine (N_2H_4): In addition to nitrite, Watt and Chrisp method [12] is used to detect the by-product N_2H_4. 0.998 g $C_9H_{11}NO$, 5 mL HCl and 50 mL ethanol are mixed as the color reagent. Firstly, a series of N_2H_4 standard solutions with fixed concentrations are prepared, and then 2 mL standard samples are mixed with 2 mL chromogenic agent, respectively, and the reaction with dark lasts for 20 min. Finally, the UV-vis absorbance of the solutions after chromogenic reaction are measured at 455 nm. The standard curve of N_2H_4 is obtained by fitting different concentrations of N_2H_4 standard solution with corresponding absorbance. The concentration of N_2H_4 in electrolyte with unknown concentration can be calculated by measuring its absorbance at 455 nm and plugging it into a standard curve.

Determination of hydrogen (H_2): In the NO_3^-RR process, there is a competitive reaction HER in cathode. H_2 is the product of HER process and can be detected by blowing the product after electrolysis in the cathode chamber into a gas chromatograph (GC). In order to reduce the experimental error caused by the different thermal conductivity of the gas, the carrier gas of the chromatography is nitrogen. Nitrogen is

passed into the cathode electrolyte at a flowing rate of 30 mL min^{-1}, and GC collected the gas produced by the reaction in the cathode chamber every 5 minutes. The hydrogen concentration can be obtained by integrating the characteristic peaks of hydrogen collected in the TCD detector.

Calculations of faradaic efficiency (FE) and yield rate: The yields of NH_3 and NO_2^- are calculated by equation (4):

$$Yield = C \times V \div (t \times m_{cat.}) \quad (4)$$

The FE of NH_3 is calculated by equation (5):

$$FE_1 = 8 \times F \times C(NH_3) \times V \div (17 \times Q) \quad (5)$$

The FE of NO_2^- is calculated by equation (6):

$$FE_2 = 2 \times F \times C(NO_2^-) \times V \div (46 \times Q) \quad (6)$$

The concentration of H_2 is measured by GC and TCD. The volume mole number n can be calculated according to formula (7):

$$n = P \times V' \div (R \times T) \quad (7)$$

The corresponding FE of H_2 can be calculated by equation (8):

$$FE_3 = n \times [H_2] \times F \times 2 \div Q \quad (8)$$

where C is the measured NH_3/NO_2^- concentration, V the volume of electrolyte in the cathode chamber, t the time for which the potential is applied, $m_{cat.}$ the mass of catalyst loaded on the working electrode, F the Faraday constant (F=96485 C mol^{-1}), Q the charge applied, P the standard atmospheric pressure, V' the volume of gas through GC, R the universal gas constant, T the reaction temperature.

^{15}N isotope labeling experiments

$Na^{15}NO_3$ is used as N source for nitrate reduction isotope labeling experiment to verify the origin of as-synthesized ammonia. The purity of $Na^{15}NO_3$ is more than 98.5% and they are stored in a vacuum drying oven before being used. 0.1 M $Na^{15}NO_3$+0.1 M KOH as the electrolyte, the catalyst is subjected to $^{15}NO_3$RR for 20 h at the optimum voltage. To prepare the NMR sample, the pH of the electrolyte is adjusted to about 3 with 0.5 M H_2SO_4, then 0.5 mL electrolyte is added with 0.01 vol% DMSO and 0.1 mL D_2O, respectively. And the ^{1}H NMR spectrum of $^{15}NH_4^+$ (400 MHz) is determined. As a control, ^{1}H NMR spectrum is tested after reaction in 0.1 M $Na^{14}NO_3$+0.1 M KOH electrolyte.

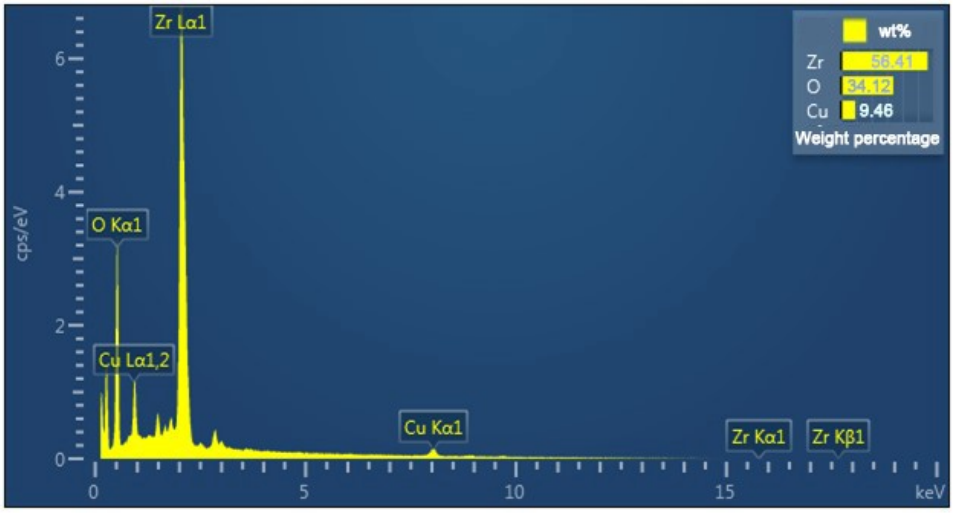

Fig. S1. EDS pattern of the CDZ.

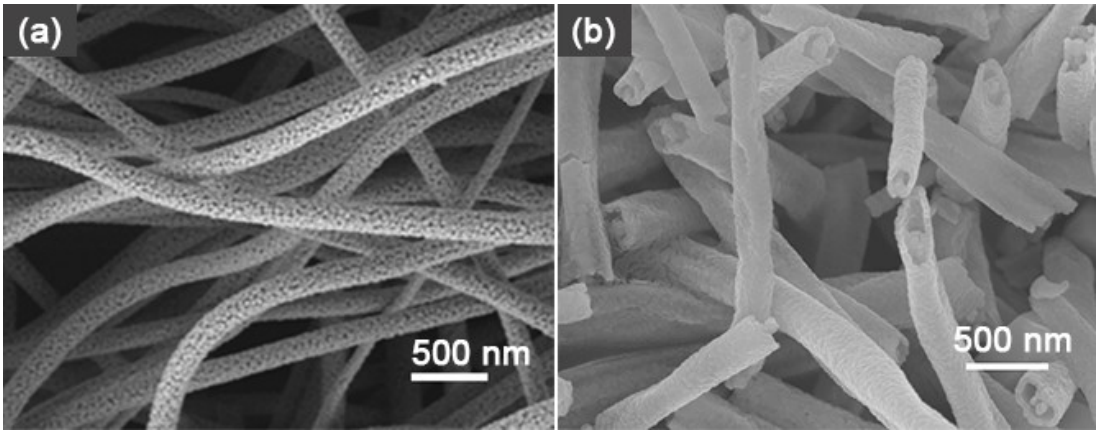

Fig. S2. SEM images of the (a) ZrO_2 and (b) CDZ.

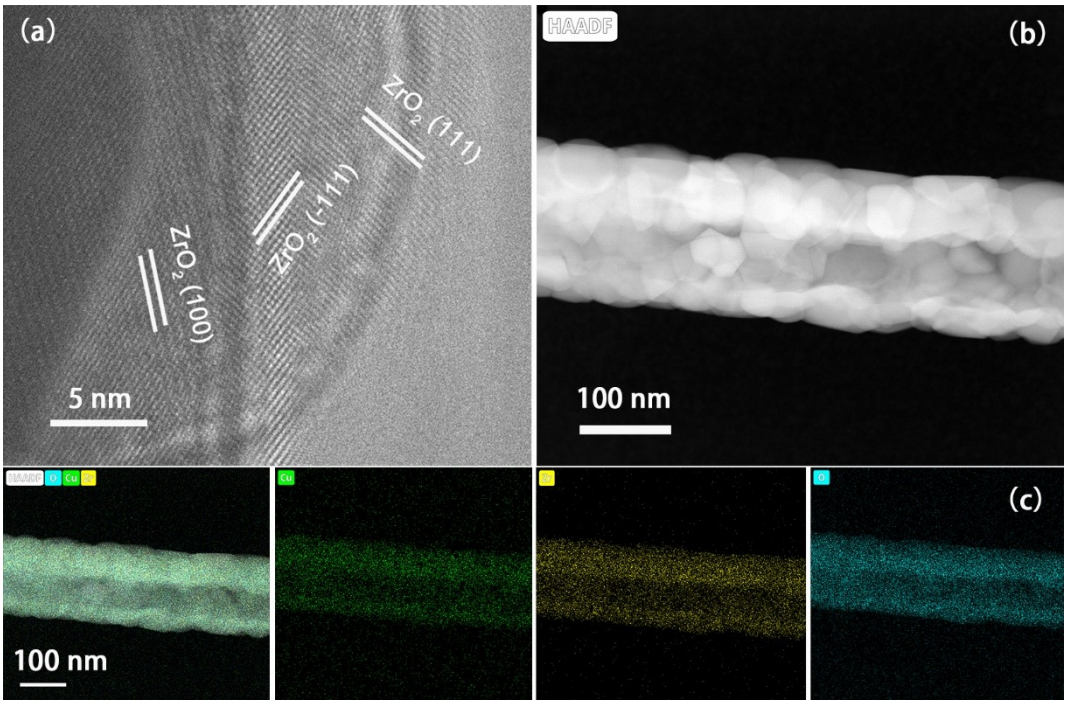

Fig. S3. (a) HRTEM image of CDZ, (b) TEM image of CDZ and (c) elemental mapping of Cu, Zr, O in CDZ.

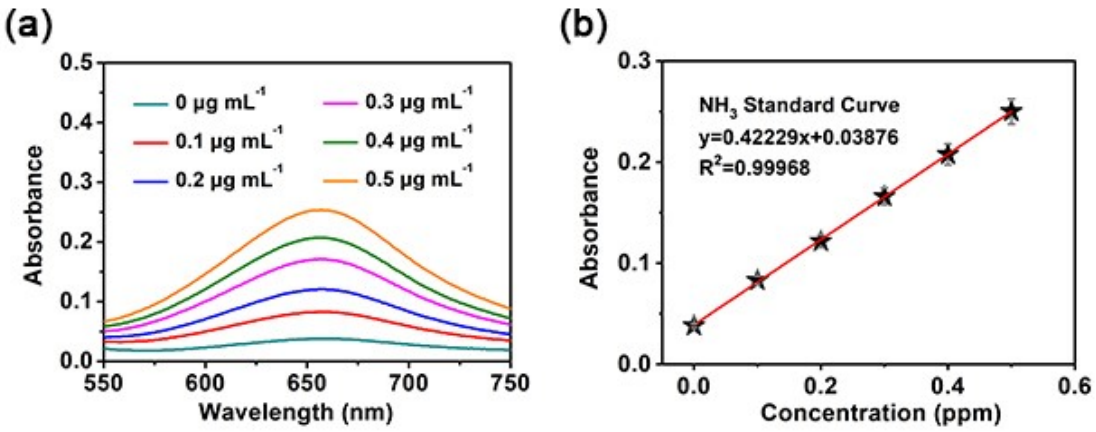

Fig. S3. (4) UV-vis absorption spectra of different concentrations of NH_3 stained with indophenol blue and (b) the corresponding calibration curve in 0.1 M KOH.

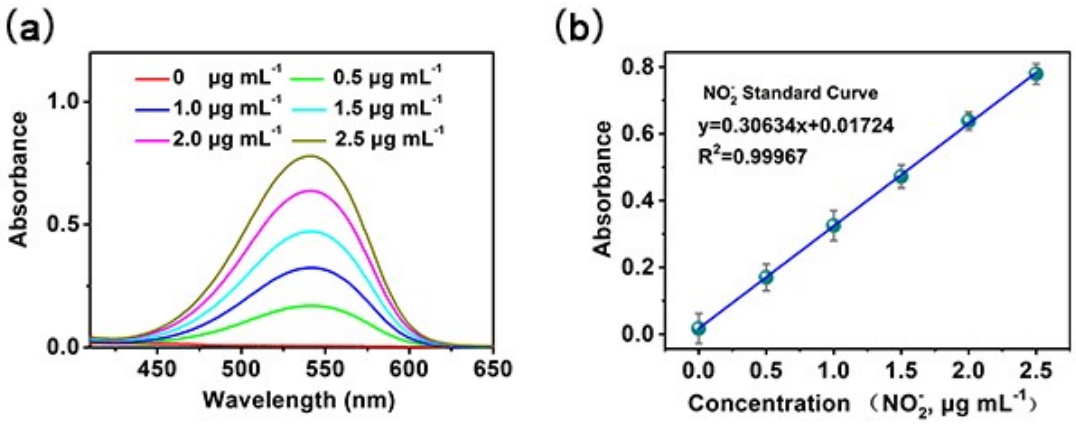

Fig. S5. (a) UV-vis absorption spectra of various concentrations of NO_2^- after sitting for 20 minutes and (b) the corresponding calibration curve in 0.1 M KOH.

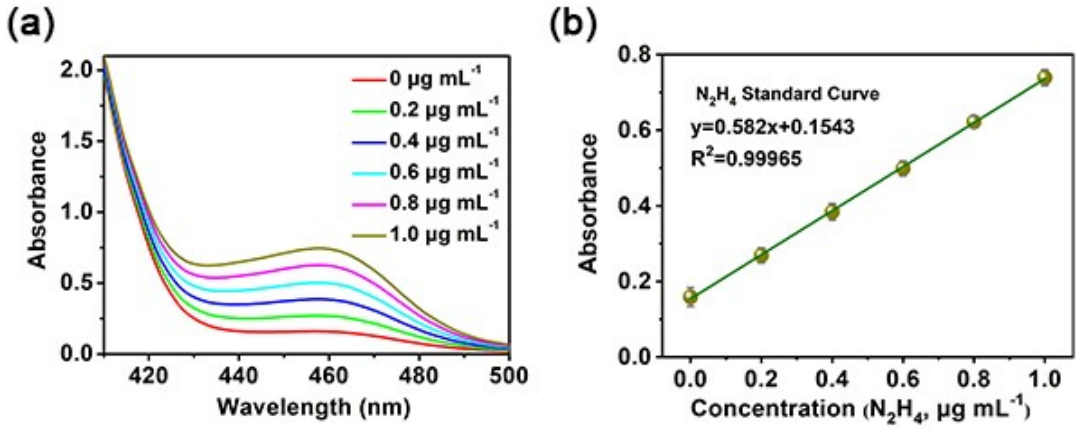

Fig. S6. (a) UV-vis absorption spectra of different concentrations of N_2H_4 stained by Watt and Chrisp method and (b) the corresponding calibration curve in 0.1 M KOH.

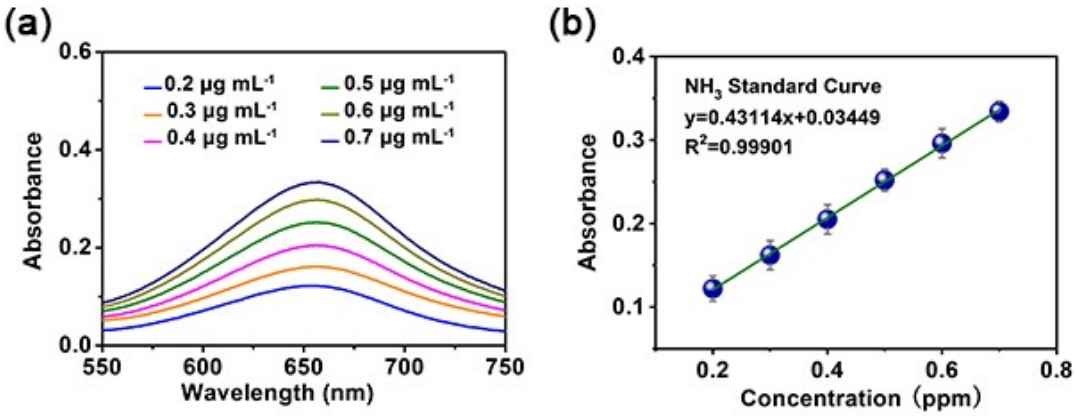

Fig. S7. (a) UV-vis absorption spectra of different concentrations of NH_3 stained with indophenol blue and (b) the corresponding calibration curve in 0.1 M PBS.

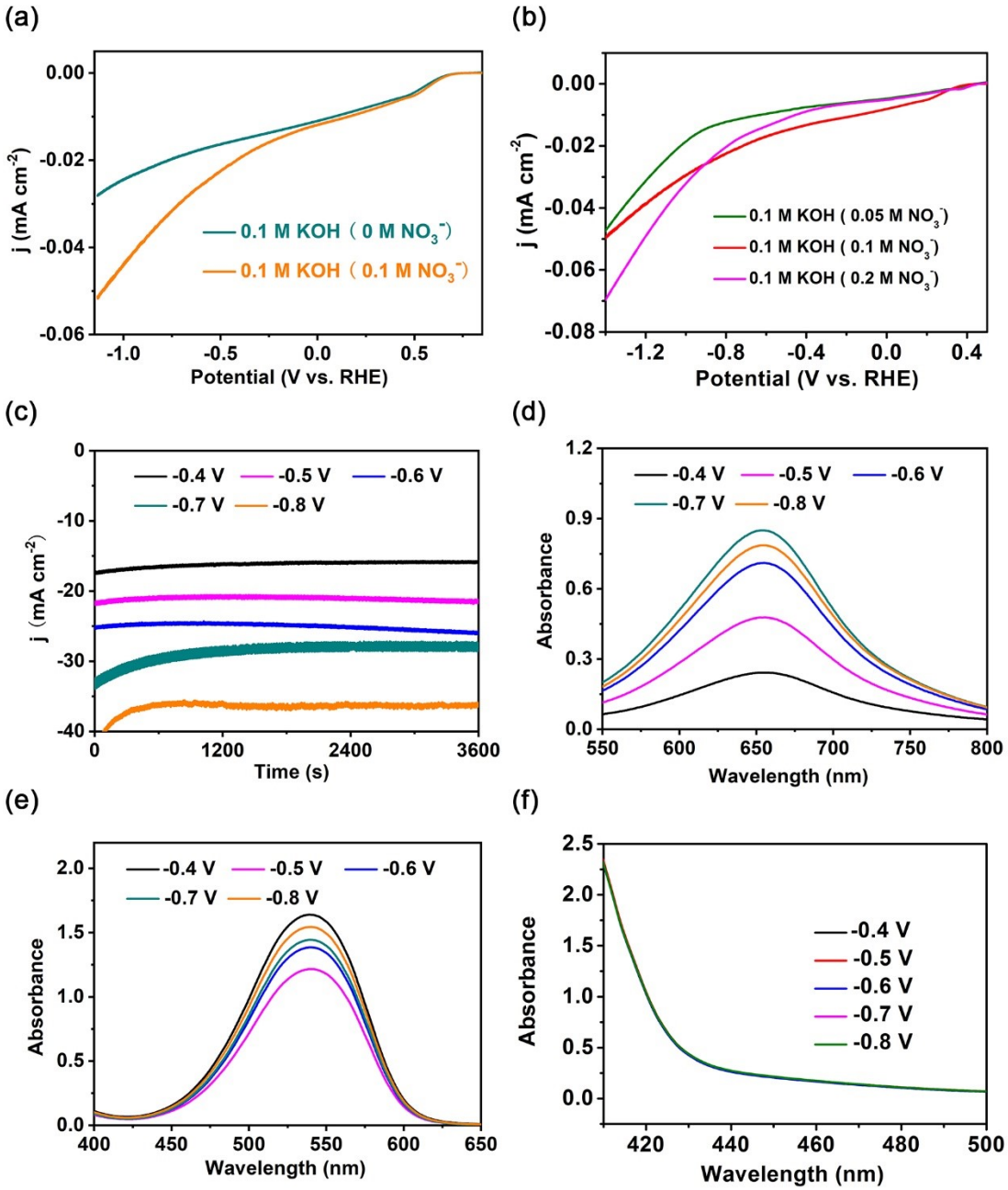

Fig. S8. (a) LSV curves in 0.1 M KOH and 0.1 M KOH+0.1 M $NaNO_3$ for CLZ. (b) LSV curves in 0.1 M KOH electrolytes containing different concentrations of nitrate for CLZ. (c) i-t curves at different potentials in 0.1 M KOH+0.1 M $NaNO_3$. UV-vis absorption spectra of (d) NH_3, (e) NO_2^- and (f) N_2H_4. Note that the electrolytes obtained at all potentials are diluted 20 times. As for the NO_2^- tests, the electrolytes obtained at all the potentials are diluted 10 times.

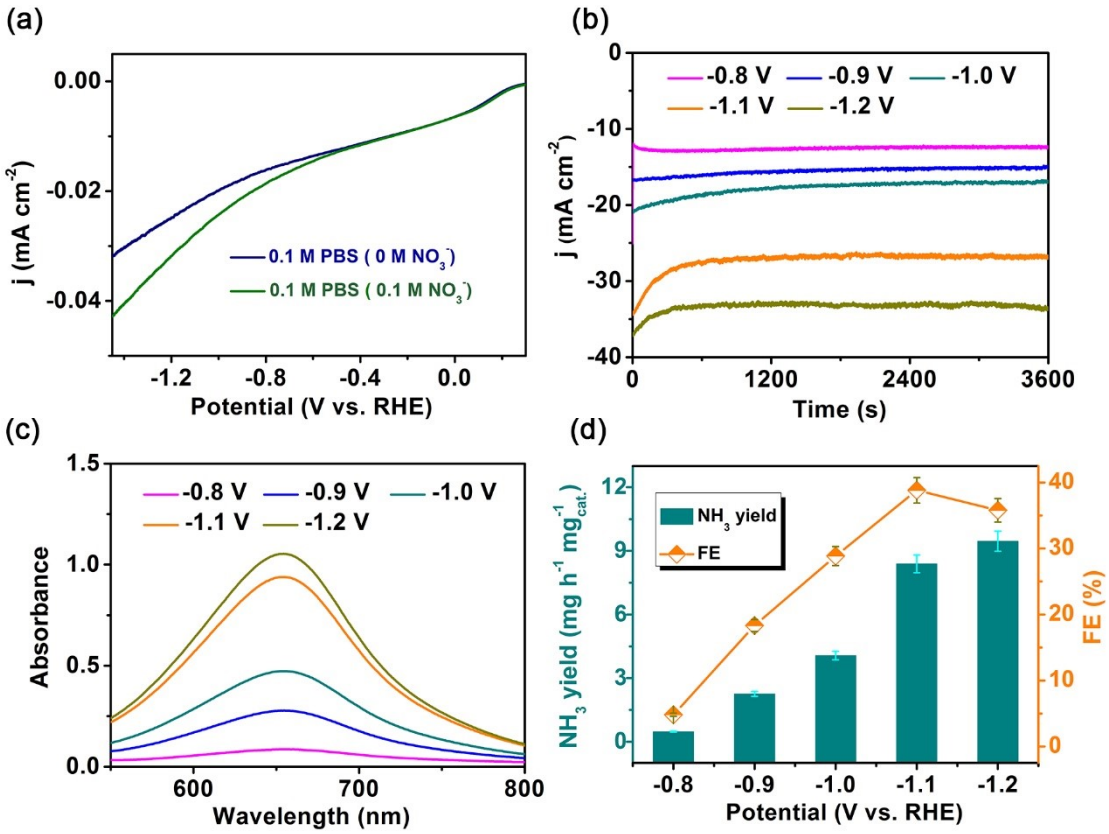

Fig. S9. (a) LSV curves in 0.1 M PBS and 0.1 M PBS+0.1 M $NaNO_3$ for CLZ. (b) i-t curves for 1 h, (c) UV-vis absorption spectra of NH_3 and (d) NH_3 yields and FEs at different potentials in 0.1 M PBS+0.1 M $NaNO_3$ for CLZ. Note that the electrolytes obtained at all potentials are diluted 10 times.

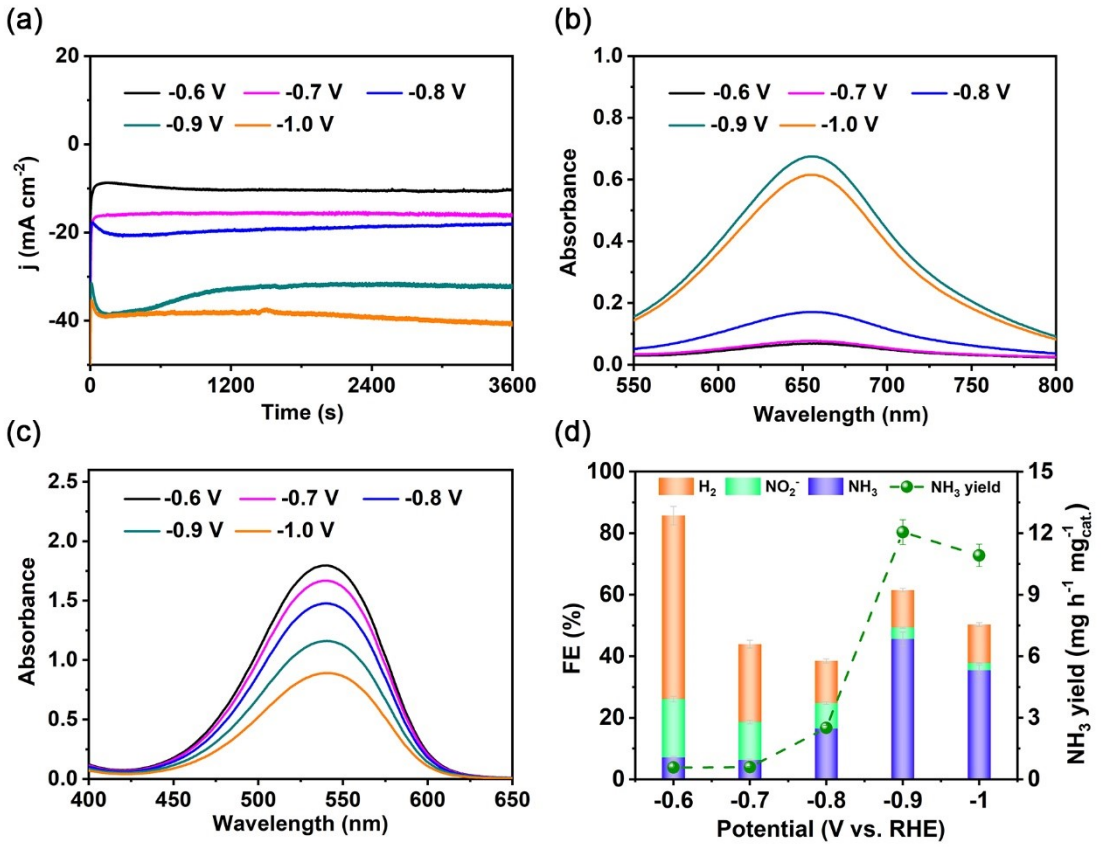

Fig. S10. (a) i-t curves for 1 h, (b) UV-vis absorption spectra of NH_3, (c) UV-vis absorption spectra of NO_2^- and (d) NH_3 yields and FEs at different potentials in 0.1 M KOH+0.1 M $NaNO_3$ for ZrO_2. Note that the electrolytes obtained at all potentials are diluted 20 times. As for the NO_2^- tests, the electrolytes obtained at all the potentials are diluted 10 times.

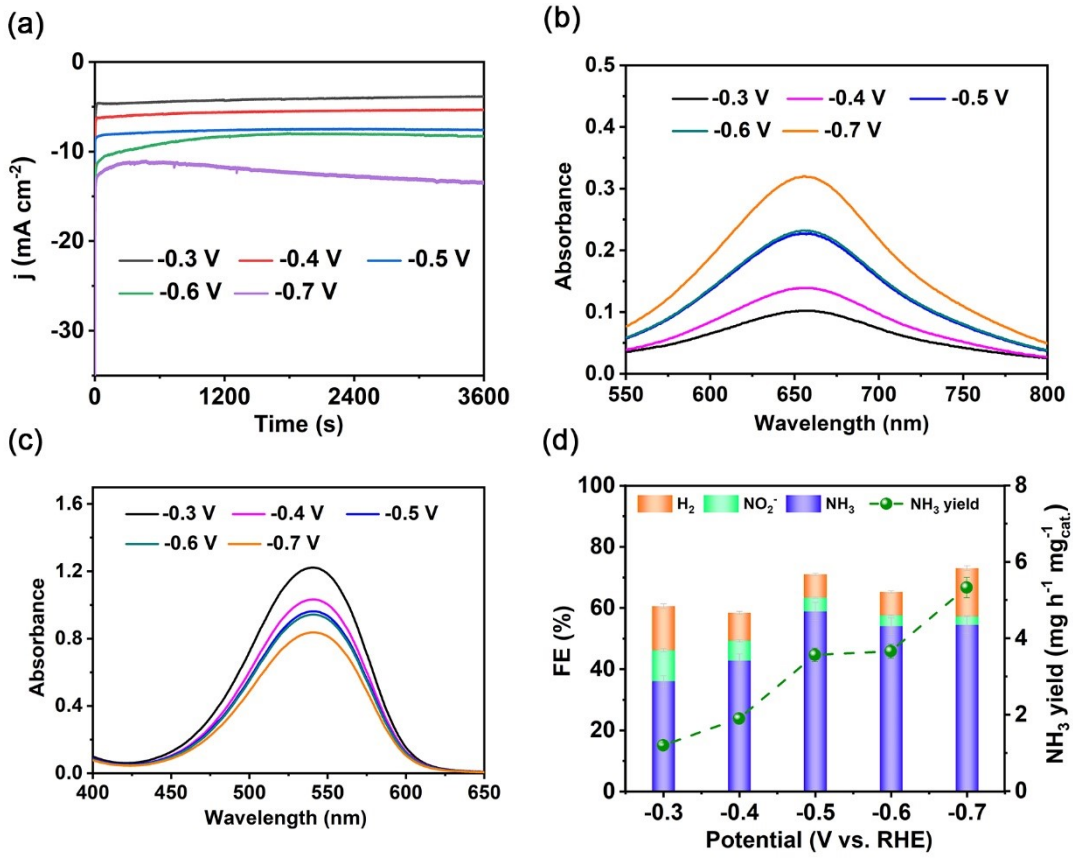

Fig. S11. (a) i-t curves for 1 h, (b) UV-vis absorption spectra of NH_3, (c) UV-vis absorption spectra of NO_2^- and (d) NH_3 yields and FEs at different potentials in 0.1 M KOH+0.1 M $NaNO_3$ for CDZ. Note that the electrolytes obtained at all potentials are diluted 20 times. As for the NO_2^- tests, the electrolytes obtained at all the potentials are diluted 10 times.

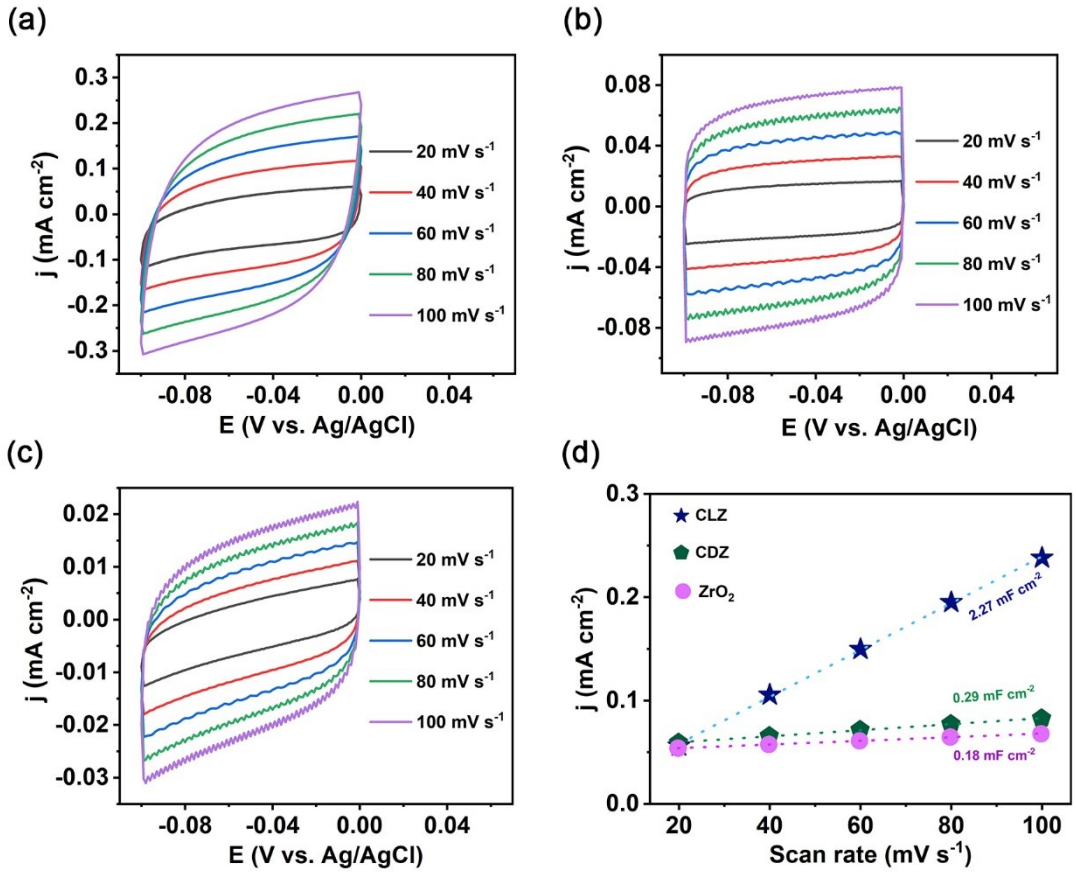

Fig. S12. (a-c) CV curves of different scan rates of ZrO_2, CDZ and CLZ. (d) The corresponding double layer capacitance.

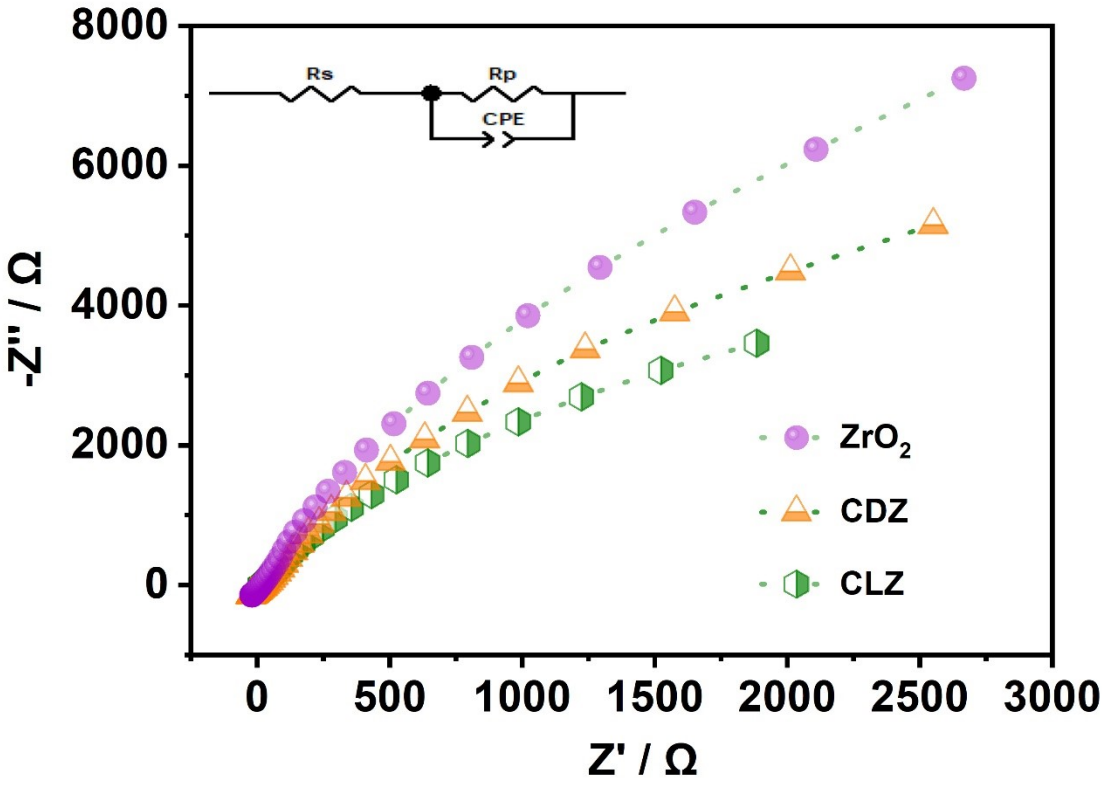

Fig. S13. Electrochemical spectra impedance of ZrO_2, CDZ and CLZ with an equivalent circuit.

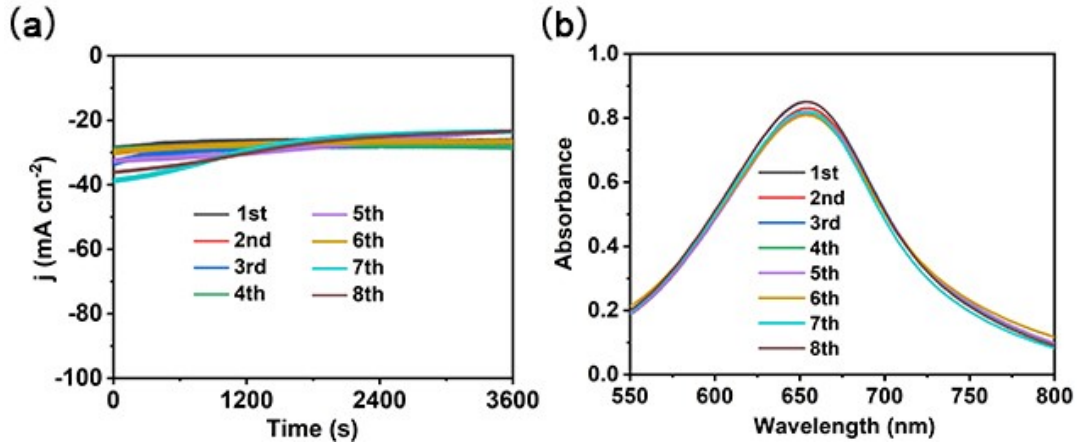

Fig. S14. (a) i-t curves for 1 h and (b) UV-vis absorption spectra of NH_3 for 8 consecutive cycles in 0.1 M KOH+0.1 M $NaNO_3$ for CLZ. Note that the electrolytes obtained at all potentials are diluted 20 times.

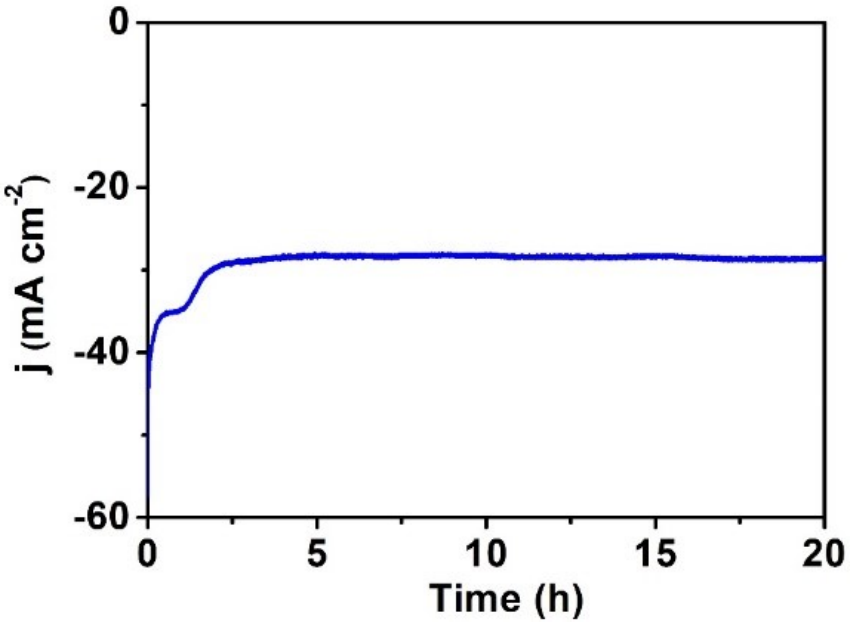

Fig. S15. Chronoamperometric test for CLZ at -0.7 V for 20 h.

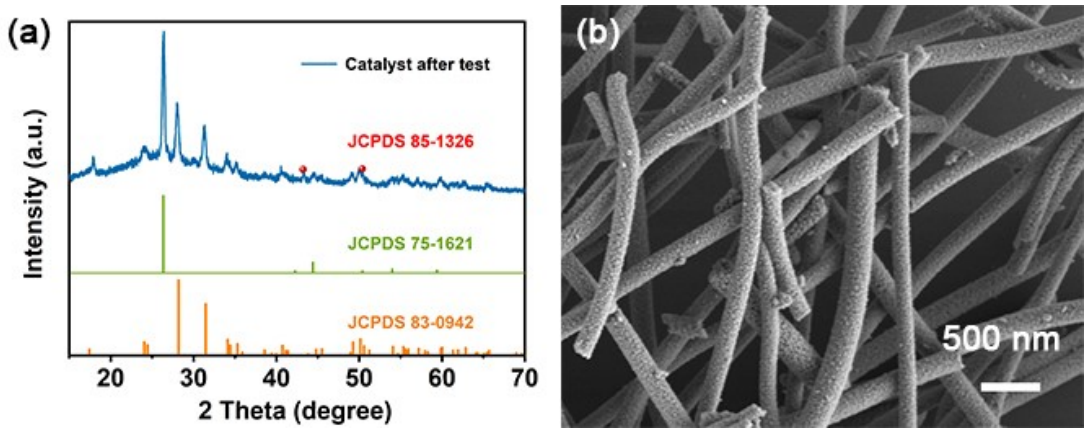

Fig. S16. (a) XRD pattern and (b) SEM image of CLZ after 20-h electrolysis at -0.7 V.

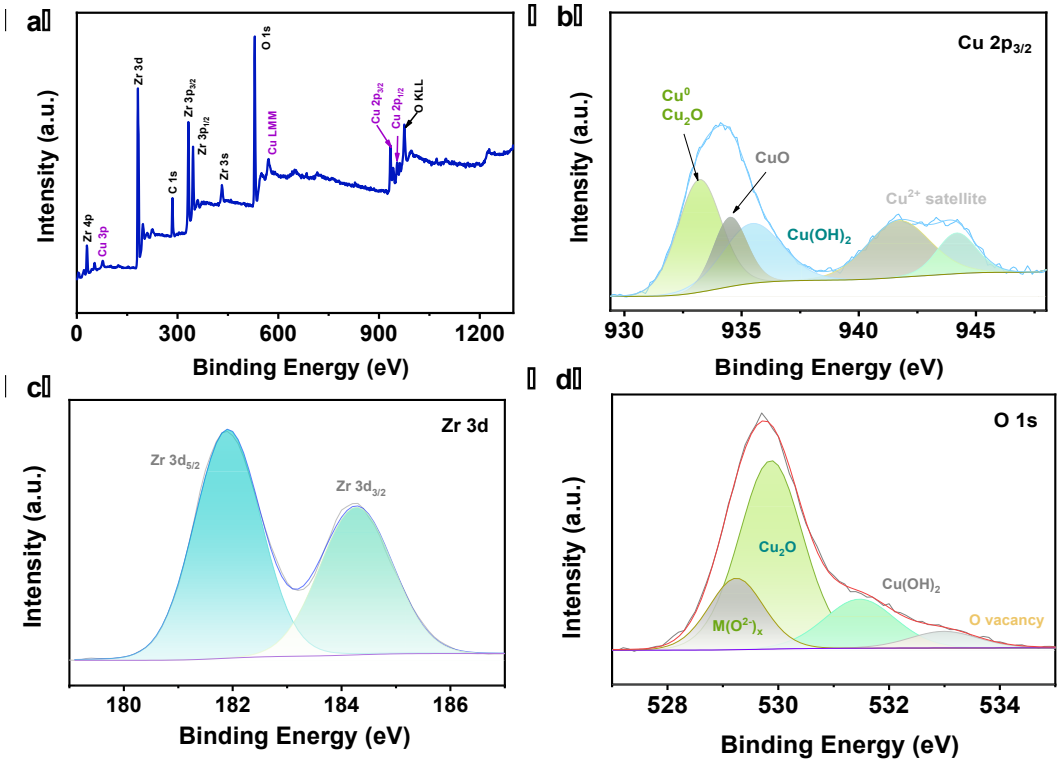

Fig. S17. (a) XPS survey spectrum, (b) Cu $2p_{3/2}$ XPS spectra, (c) Zr 3d XPS and (d) O 1s XPS spectra of CLZ after 2-h electrolysis at -0.7 V.

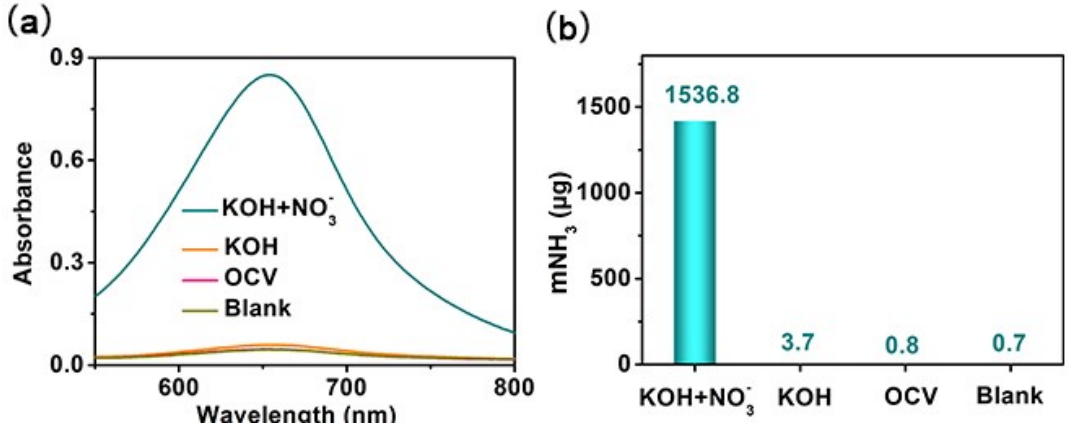

Fig. S18. (a) UV-vis absorption spectra of indophenol assays and (b) corresponding ammonia yield after 1-h electrolysis under different condition for CLZ.

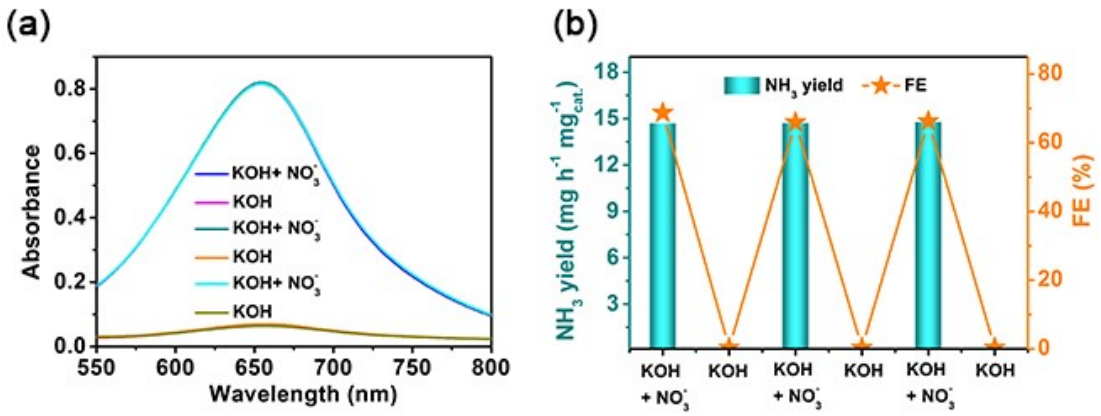

Fig. S19. (a) UV-vis absorption spectra of NH_3 and (b) NH_3 yields and FEs with alternating 1 h cycles in the KOH electrolyte with and without $NaNO_3$ for CLZ.

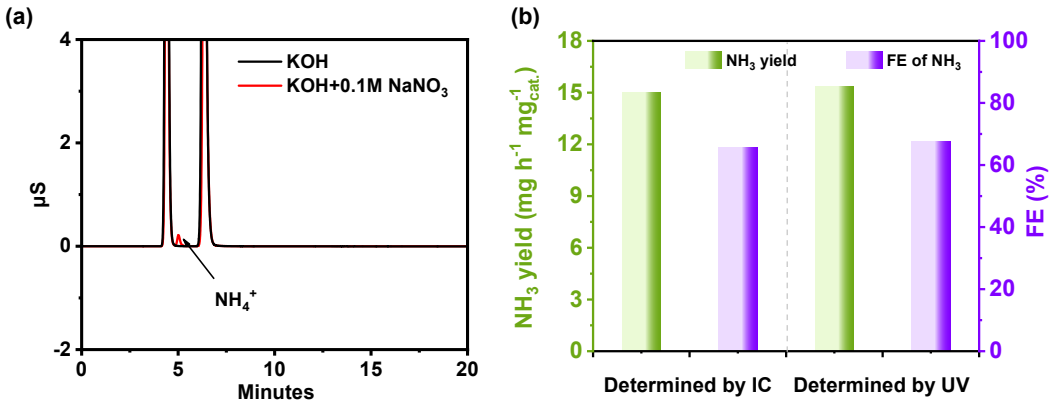

Fig. S20. (a) Ion chromatogram (IC) and (b) the ammonia yield rate and FE using IC method and UV method after 1-h electrolysis in 0.1 M KOH+0.1 M $NaNO_3$ at -0.7 V for CLZ.

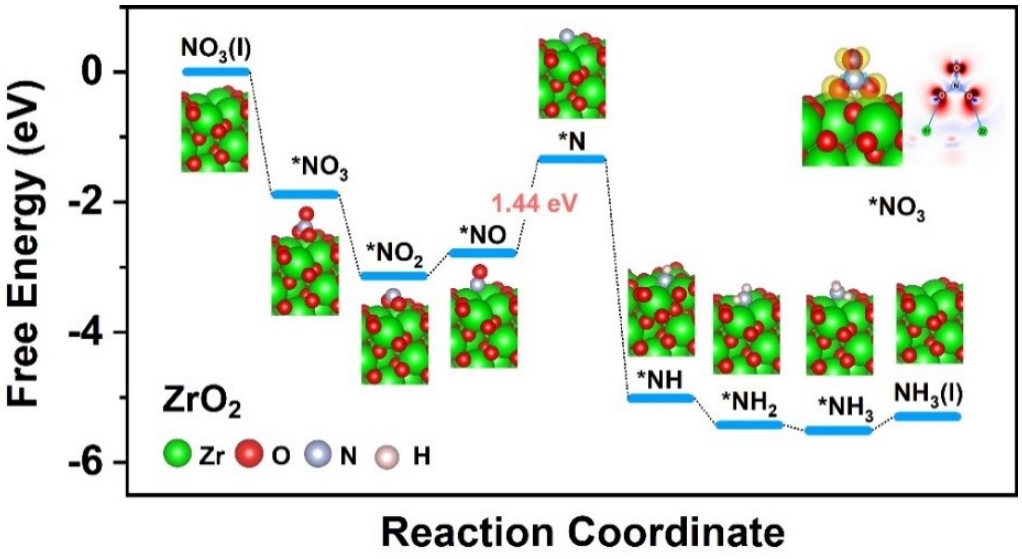

Fig. S21. Calculated free energy changes of NO_3^-RR at the ZrO_2 surface.

Table S1 Comparison of electrocatalytic production of ammonia performance for CLZ with other electrocatalysts under ambient conditions.

Catalyst	Starting species	Electrolyte	Yield of NH_3 ($\mu g\ h^{-1}\ cm^{-2}$/ $\mu g\ h^{-1}\ mg^{-1}$)	FE(%)	Ref.
CLZ	**NO_3^-**	**0.1 M KOH**	**-/15368.4**	**67.6**	**This work**
CDZ	**NO_3^-**	**0.1 M KOH**	**-/3566.1**	**58.9**	**This work**
ZrO_2	**NO_3^-**	**0.1 M KOH**	**-/12053.14**	**45.6**	**This work**
CuPc-GCE	NO_3^-	0.1 M KOH	/	64.0	[13]
Cu nanosheets	NO_3^-	0.1 M KOH	-/390.1	99.7	[14]
Co_3O_4@NiO HNTs	NO_3^-	0.5 M Na_2SO_4	-/117.8	54.9	[15]
Cu-PTCDA	NO_3^-	0.1 M PBS	436/-	85.9	[16]
Cu nanodisks	NO_3^-	0.1 M KOH	-/2160	81.1	[17]
CoP NA/TM	NO_3^-	0.1 M PBS	2260.7/-	90.0	[18]
Cu-ZrO_2	N_2	0.1 M Na_2SO_4	-/12.13	13.4	[19]
ZrO_2	N_2	0.1 M Na_2SO_4	-/9.63	12.1	[9]

C@YSZ	N_2	0.1 M Na_2SO_4	-/24.6	8.2	[20]

References

1. G. Kresse and J. Furthmüller, *Comp. Mater. Sci.*, 1996, **6**, 15-50.
2. G. Kresse and J. Hafner, *Phys. Rev. B*, 1994, **49**, 14251.
3. G. Kresse and J. Furthmuller, *Phys. Rev. B*, 1996, **54**, 11169-11186.
4. P. E. Blöchl, *Phys. Rev. B*, 1994, **50**, 17953.
5. J. P. Perdew, J. A. Chevary, S. H. Vosko, K. A. Jackson, M. R. Pederson, D. J. Singh and C. Fiolhais, *Phys. Rev. B*, 1992, **46**, 6671.
6. S. Grimme, J. Antony, S. Ehrlich and H. Krieg, *J. Chem. Phys.*, 2010, **132**, 154104.
7. H. J. Monkhorst and J. D. Pack, *Phys. Rev. B*, 1976, **13**, 5188.
8. J. Norskov, J. Rossmeisl, A. Logadottir, L. Lindqvist, J. Kitchin, T. Bligaard and H. Jonsson, *J. Phys. Chem. B*, 2004, **108**, 17886-17892.
9. J. Xia, H. Guo, M. Cheng, C. Chen, M. Wang, Y. Xiang, T. Li and E. Traversa, *J. Mater. Chem. A*, 2021, **9**, 2145-2151.
10. D. Zhu, L. Zhang, R. E. Ruther and R. J. Hamers, *Nat. Mater.*, 2013, **12**, 836-841.
11. L. C. Green, D. A. Wagner, J. Glogowski, P. L. Skipper, J. S. Wishnok and S. R. Tannenbaum, *Anal. Biochem.*, 1982, **126**, 131-138.
12. G. W. Watt and J. D. Chrisp, *Anal. Chem.*, 1952, **24**, 2006-2008.
13. N. Chebotareva and T. Nyokong, *J. Appl. Electrochem.*, 1997, **27**, 975-981.
14. X. Fu, X. Zhao, X. Hu, K. He, Y. Yu, T. Li, Q. Tu, X. Qian, Q. Yue, M. R. Wasielewski and Y. Kang, *Appl. Mater. today*, 2020, **19**, 100620.
15. Y. Wang, C. Liu, B. Zhang and Y. Yu, *Sci. China Mater.*, 2020, **63**, 2530-2538.
16. G.-F. Chen, Y. Yuan, H. Jiang, S.-Y. Ren, L.-X. Ding, L. Ma, T. Wu, J. Lu and H.

Wang, *Nat. Energy*, 2020, **5**, 605-613.

17. K. Wu, C. Sun, Z. Wang, Q. Song, X. Bai, X. Yu, Q. Li, Z. Wang, H. Zhang, J. Zhang, X. Tong, Y. Liang, A. Khosla and Z. Zhao, *ACS Mater. Lett.*, 2022, **4**, 650.
18. G. Wen, J. Liang, Q. Liu, T. Li, X. An, F. Zhang, A. A. Alshehri, K. A. Alzahrani, Y. Luo, Q. Kong and X. Sun, *Nano Res.*, 2022, **15**, 972-977.
19. T. Li, J. Xia, Q. Chen, K. Xu, Y. Gu, Q. Liu, Y. Luo, H. Guo and E. Traversa, *ACS Appl. Mater. Inter.*, 2021, **13**, 40724-40730.
20. S. Luo, X. Li, M. Wang, X. Zhang, W. Gao, S. Su, G. Liu and M. Luo, *J. Mate. Chem. A*, 2020, **8**, 5647-5654.